ELSEVIER

International Journal of Mass Spectrometry 177 (1998) 1–15

International Journal of Mass Spectrometry

Pulsation phenomena during electrospray ionization

R. Juraschek, F.W. Röllgen*

Institut für Physikalische und Theoretische Chemie, Universität Bonn, Wegelerstr. 12, D-53115 Bonn, Germany

Received 16 January 1998; accepted 6 April 1998

Abstract

Capillary current pulsations appearing under conditions of electrospray mass spectrometry and their dependence on the disintegration of an H_2O/MeOH solution at the end of the capillary have been investigated by combining measurements of the capillary current with optical microscopy of the disintegration of the liquid at the capillary tip. With increasing capillary potential two pulsating and one continuous axial spray mode could be distinguished. Pulsations with frequencies in the low kilohertz range are related to a transient emission of liquid via a cone jet and are caused by an imbalance between the emission rate of liquid and its supply rate to the apex of the cone. Low frequency pulsations of a sequence of emission pulses are due to an imbalance between the supply of liquid to the cone volume and its loss by a sequence of emission pulses. A mechanism of the disintegration of the jet into charged droplets is proposed. The dependence of the pulsations on the flow rate, electrolyte concentration, surface tension, and capillary diameter is shown. Mass spectrometry revealed that high ion signal intensities are obtained at higher capillary potentials in the continuous axial spray mode and at lower capillary potentials in the transition range between the two pulsating axial spray modes because of the formation of small highly charged droplets. In experiments with nanoelectrospray capillaries, current pulsations were observed only after the onset of a (corona) discharge. (Int J Mass Spectrom 177 (1998) 1–15) © 1998 Elsevier Science B.V.

Keywords: Electrospray ionization; Cone jet; Pulsation phenomena

1. Introduction

Electrospray mass spectrometry (ESMS) has become a widely accepted and very useful tool in biochemical analysis since its first introduction in 1984 by Yamashita and Fenn [1] and Alexandrov et al. [2]. Nevertheless, a lack of detailed understanding of the electrospray ionization (ESI) mechanism still impedes a rational choice of experimental parameters. The ESI process can be divided in two consecutive steps. First, the electrohydrodynamic disintegration of an electrolyte-containing solution at atmospheric pressure into charged droplets and second, the release of ions from charged droplets. The second step is subject to a controversial discussion [3–9]. In our view it is fairly well understood that charged droplets decompose below the Rayleigh limit via ellipsoidal deformations and uneven fissions into smaller droplets up to a size where solvent evaporation without further electrohydrodynamic disintegration processes releases ions into the gas phase [10]. The first step in ESI is less understood.

Electrospraying of liquids is used in a number of techniques such as crop and paint spraying and ink jet printing. It has been a subject of research in aerosol science for a rather long time [11]. However, these investigations are related to rather different conditions

* Corresponding author.

PII S1387-3806(98)14025-3

compared with those met in ESMS so that the results often provide only limited information. Spray modes appearing in electrohydrodynamic spraying of liquids have been reviewed by Grace and Marijnissen [12] and by Cloupeau and Prunet-Foch [13].

Optical observations of the electrohydrodynamic disintegration of liquids under ESMS conditions showed the appearance of different spray modes. In the "axial spray mode" (also called *cone jet mode*), the liquid issuing from the capillary tip forms a cone, at the apex of which a liquid filament ("jet") is emitted. Further downstream the jet becomes unstable and disperses into a mist of charged fine droplets. Under these conditions, pulsation phenomena (i.e. the appearance and disappearance of the liquid jet) could be observed within the time resolution of a video system used [14]. Such pulsation phenomena have frequently been reported in the literature [13,15–18]. Recently, Charbonnier et al. [19] reported pulsations of capillary currents in the higher kilohertz range during ESI, which raised the question of a correlation between the observed current pulses and the disintegration of the liquid. Such a correlation might be used to distinguish and characterize different spray modes by their current characteristics. It might also be helpful to optimize the electrospray process with respect to the achievement of a high ion yield for mass analysis, because different sizes of droplets generated in the different spray modes can be expected. A high ion yield is favored by the disintegration of the analyte solution into small droplets.

The present paper reports investigations on the origin of capillary current pulsations during ESI and their correlation with the disintegration of the liquid at the end of the capillary. To this end we combined measurements of the capillary current with optical microscopy and flash photography of the disintegration of the liquid. Furthermore, we investigated the dependence of the current pulsations on experimental parameters that are typically varied in ESMS.

2. Experimental

The experimental setup used in the main part of this study is shown schematically in Fig. 1. The high

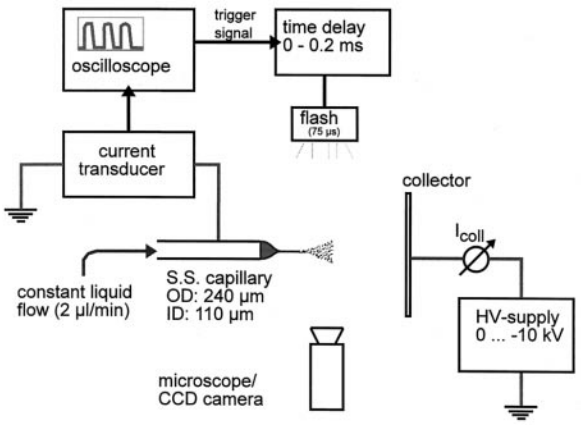

Fig. 1. Schematic diagram of the experimental setup for optical observation and monitoring the capillary current in ESI.

electrical potential is applied between the collector, a stainless steel plate, and the capillary at ground potential. Accordingly the capillary current transducer (Burr-Brown, Tucson, AZ, model 3554, gain-bandwidth product, 1.7 GHz) had to not be floated above ground potential. The current was monitored by means of a storage-oscilloscope or optionally by a spectrum analyzer. With this setup, current pulsations with amplitudes in the nanoampere range could be resolved up to frequencies of ~1 MHz. In addition to the time-resolved measurements of the capillary current, the average current at the collector was also recorded.

The renunciation of mass analysis and therefore of an atmospheric pressure interface to a mass analyzer allowed effective shielding of the setup against interfering electric fields and facilitated the optical observations. For optical investigations a stereo-zoom microscope equipped with a CCD video camera was used. The capillary tip region was either continuously illuminated or illuminated by a flashlight (flash duration ~75 μs). The flashlight was triggered by a signal from the oscilloscope with an adjustable time delay to a periodic event. This allowed us to optically observe a complete cycle of a periodic liquid emission process with a series of snapshots.

A 10-cm-long stainless steel capillary with a blunt tip, inner diameter (i.d.) of 110 μm, and outer diameter (o.d.) of 240 μm (Hamilton) was supplied with liquid through a fused silica capillary by a glass

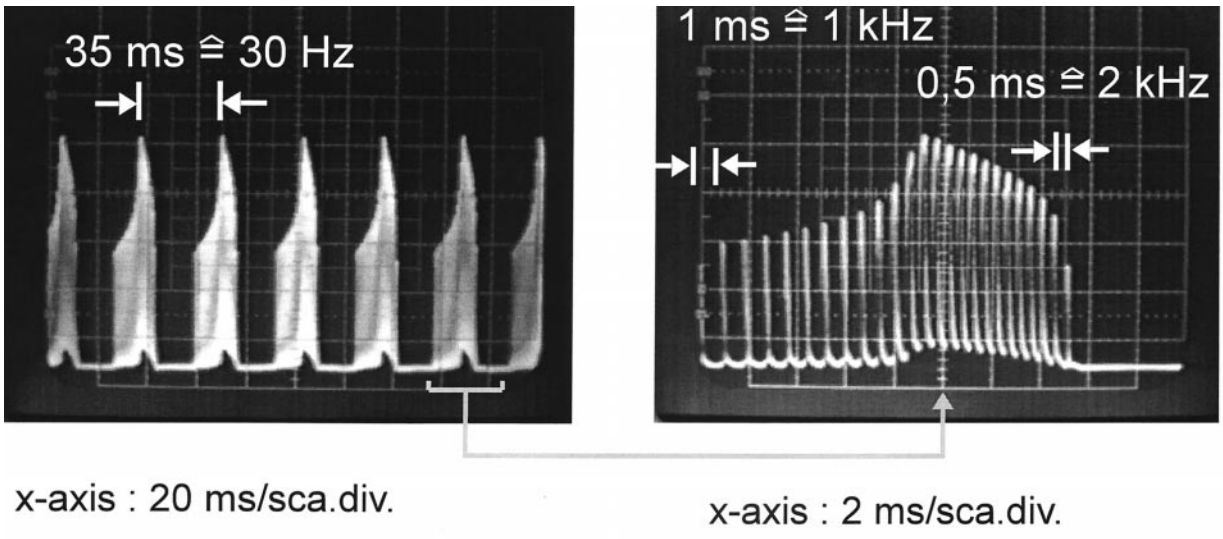

Fig. 2. Capillary current vs. time oscillograms obtained in the axial spray mode I with H_2O/MeOH (volume ratio 1:1), U_{cap} = 2.1 kV and I_{coll} = 15 nA; *y* axis, 20 nA/div.

syringe driven by a syringe pump at a constant flow rate of 2 μL/min, unless otherwise noted. For the investigations of the liquid disintegration with capillaries of different diameters stainless steel capillaries with i.d./o.d. of 60/160 μm, 180/360 μm, and 150/720 μm and blunt tips (Hamilton) were used. In addition, very small capillaries, i.e. drawn glass capillaries with a defined tip diameter (i.d./o.d. 0.5/1 μm) and tip shape (so-called Femtotip, Eppendorff, Hamburg), were used that were optionally coated with a thin gold layer. For these capillaries the distance between the capillary tip and the collector was 2 mm.

For the ESMS experiments a home built ion source combined with a quadrupole mass analyzer (QMG 420-4, Balzers) was used. The layout of the ion source was similar to the setup used for the optical observations. However, the collector was replaced by a nozzle through which the generated ions were transferred to the mass analyzer via a three stage differential pumping interface. Because the ion source had to be kept near ground potential, a positive high voltage was applied to the spraying capillary. For this reason the capillary current transducer (which could not be floated to high voltages) had to be driven by an optoelectronic coupling device, which limited the observable frequency range to about 50 kHz and led to distortions of the current peak shape already in the lower kilohertz range.

The solutions investigated (H_2O/MeOH, volume ratio 1:1) were prepared from distilled water (Millipore) and reagent grade methanol (Aldrich). Optionally KBr (Fluka), $BaBr_2$ (Aldrich), and the nonionic surfactant Triton X-114 (Serva) were added.

3. Results and discussion

3.1. Characterization of three different axial spray modes

In ESMS, typically capillaries with an i.d. of ~0.1 mm and an o.d. of ~0.25 mm and water-methanol solutions are applied. For these conditions, three different axial spray modes are observed with increasing capillary potential that can be distinguished by pulsation phenomena in the capillary current.

3.1.1. Axial spray mode I

The axial spray mode I is observed at lower capillary potentials and is characterized by the regular appearance of peak groups in the capillary current versus time oscillogram. Fig. 2 shows oscillograms

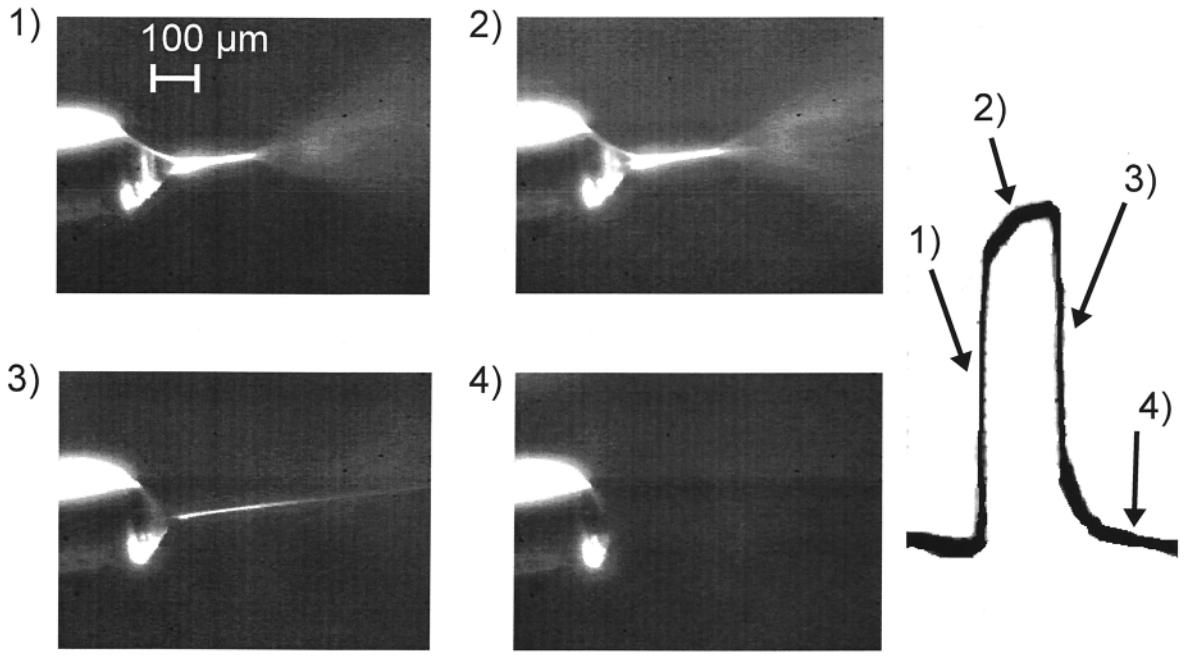

Fig. 3. Flash microphotographs of the liquid cone taken at different stages of one single current pulse at $U_{cap} = 2.4$ kV with H_2O/MeOH (1:1).

obtained with a solution of H_2O/MeOH (1:1) at a capillary potential of 2.1 kV. A current pulse sequence lasts for ~20 ms and consists of ~25 single current pulses. The sequences are separated by time intervals of ~15 ms where only a very low current is detected. Accordingly, the "low" frequency of the appearance of a pulse sequence is about 30 Hz, and single current pulses appear at "high" frequencies of 1–2 kHz. The period for the occurrence of single pulses and their amplitude varies during a pulse sequence. The period decreases from 1 ms at the beginning of a sequence to 0.5 ms at the end. The amplitude of single current pulses increases from ~50 nA at the beginning of a sequence up to ~100 nA in the middle and decreases again afterward. The duty cycle of the current emission in the axial spray mode I is roughly 20%.

Flash microphotographs taken at different stages of a single current pulse showed that a single current pulse is correlated with the emission of an axial liquid jet emerging from the apex of the cone, whereas a "relaxed" liquid cone is observed between two current pulses (Fig. 3). Obviously, single current pulses indicate a transient emission of liquid via a cone jet that accordingly appears and disappears at a "high" frequency. In the time interval between two pulse sequences the overall cone volume is small and no emission of liquid can be observed, which corresponds to the nearly vanishing capillary current (Fig. 4). The overall cone volume decreases by the emission of liquid via the formation of cone jets and increases again between the emission pulse sequences because of the continuous supply of the liquid from the capillary.

Increasing the capillary potential leads to a decrease of the time interval between the peak sequences until only high frequency pulsations are observed. In this transition range from the axial spray mode I to mode II the variation in peak shapes and in pulse repetition rates within a pulse sequence also disappear.

3.1.2. Axial spray mode II

The axial spray mode II emerges from the spray mode I by an increase of the capillary potential. This spray mode is characterized by a constant frequency

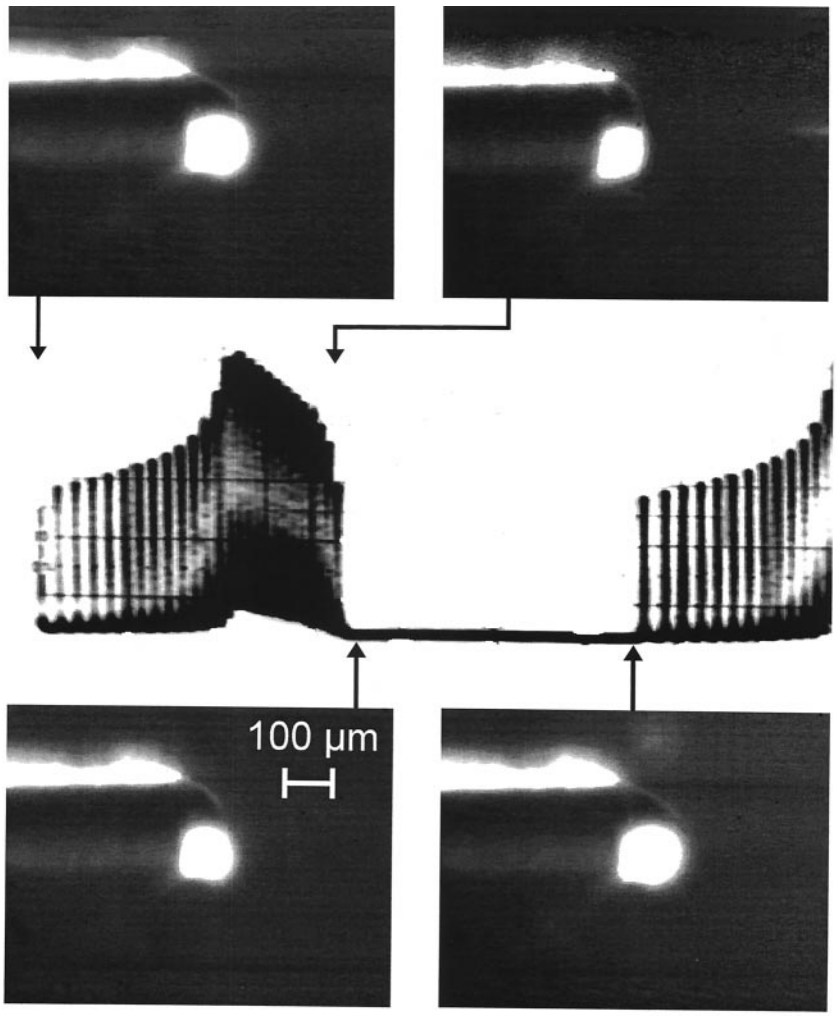

Fig. 4. Flash microphotographs of the liquid cone taken during a pulse sequence and between two pulse sequences in the axial spray mode I with H_2O/MeOH (1:1).

of the current pulsations in the lower kilohertz range and by a constant amplitude and peak shape of the pulses. This is shown in Fig. 5 for three capillary potentials. The pulsation frequency increases with increasing capillary potential (Fig. 6). The duty cycle also increases up to a limit of ~50%. If the liquid cone is continuously transluminated from the back, a darker part at the cone base can be distinguished from a brighter part at the apex of the cone (Fig. 7) where according to the duty cycle the liquid is present only about half of the time. The brighter part represents roughly 3–4% of the liquid volume of the cone and is emitted during a current pulse. This shows that a pulse cycle goes along with a rearrangement of the liquid at the cone apex.

It is interesting to note that in this spray mode the charge emitted by a single current pulse remains nearly constant (at $\sim 2.3 \times 10^{-11}$ C in the experiments of Fig. 6) and almost independent of the capillary potential applied (Fig. 6). This implies that the capillary current is linearly dependent on the pulsation frequency.

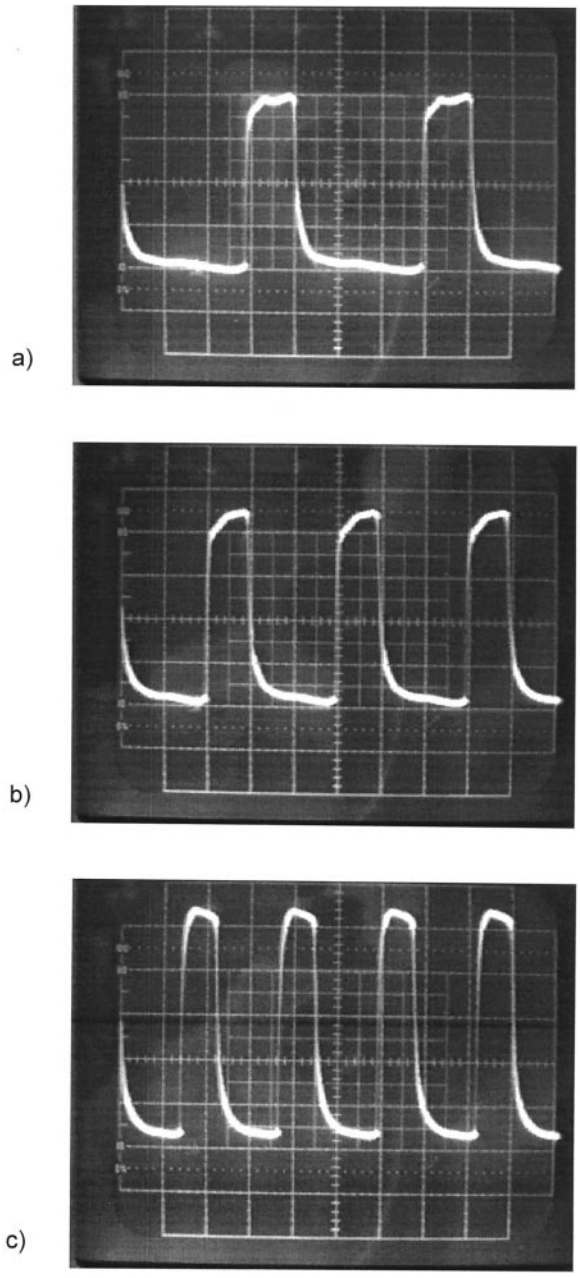

Fig. 5. Capillary current vs. time oscillograms obtained in the axial spray mode II for capillary potentials of (a) 2.25 kV, (b) 2.4 kV, and (c) 2.7 kV with H_2O/MeOH (1:1); y-axis, 20 nA/div.; x-axis, 0.2 ms/div.

If the capillary potential is raised further beyond a critical value, a sudden transition to the axial spray mode III occurs.

3.1.3. Axial spray mode III

In the axial spray mode III, which appears at higher capillary potential, a continuous emission of liquid via a cone jet is observed. With our experimental setup no current pulsations could be observed up to ~1 MHz. The oscillogramm exhibits a rather constant capillary current (Fig. 8) that is also measured at the collector. In the transition from the axial spray mode II to III an increase of the capillary current by a factor of about two is observed. This corresponds to an increase of the duty cycle of the liquid emission process from ~0.5 to 1. Optical observations confirm this result. In contrast to spray mode II, in spray mode III the whole liquid cone appears uniformly dark and stationary when it is illuminated from the back side (Fig. 9), as expected for a continuous emission process.

The shape of the cone also changes with the transition from a pulsating to the continuous spray mode. A concavely shaped cone ("cusp cone") is clearly observed in the spray modes I and II and a nearly straight cone in the spray mode III (Fig. 9). In the spray mode III the cusp shape is restricted to the apex of the cone.

3.2. Nonaxial spray modes

Further raising the capillary potential causes the transition to the "rim emission mode" [14]. In this spray mode the axial cone disappears and the liquid is emitted via several jets from the rim of the capillary. The number of jets increases with increasing capillary potential. If only two or three jets are formed with stable positions at the capillary rim, current pulsations with a corresponding number of different frequencies in the lower kilohertz range could be detected with the spectrum analyzer. It is reasonable to assume that each jet emerges from a liquid cone with a specific pulsation frequency, as was already observed for conditions of electrohydrodynamic mass spectrometry (EHMS) [20]. The liquid emission via these jets, whose number and location at the rim of the capillary change frequently, was not investigated in more detail.

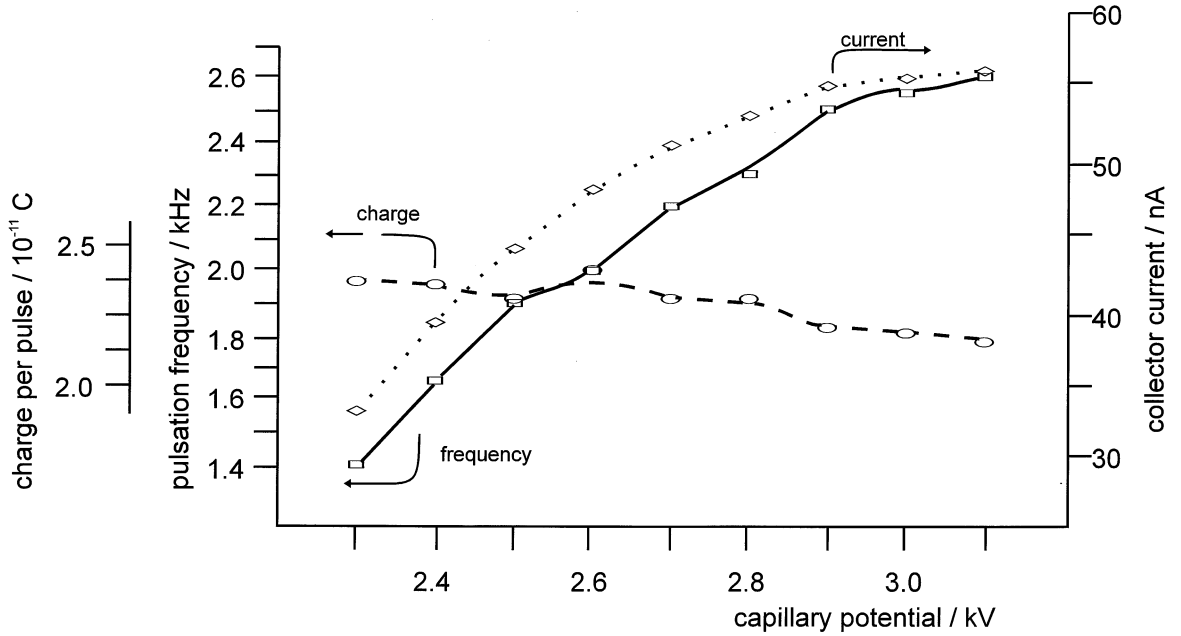

Fig. 6. Pulsation frequency, (average) collector current, and charge per pulse vs. capillary potential in the axial spray mode II with H_2O/MeOH (1:1).

3.3. Origin of the pulsation phenomena

In the axial spray mode I "low" and "high" frequency pulsations of the emission of liquid via a cone jet occur, whereas in the axial spray mode II only "high" frequency pulsations are observed. These different kinds of pulsations arise from an imbalance between the loss of liquid via emission and its supply into different regions of the liquid cone. In a "low" frequency pulsation cycle the largest part of the cone

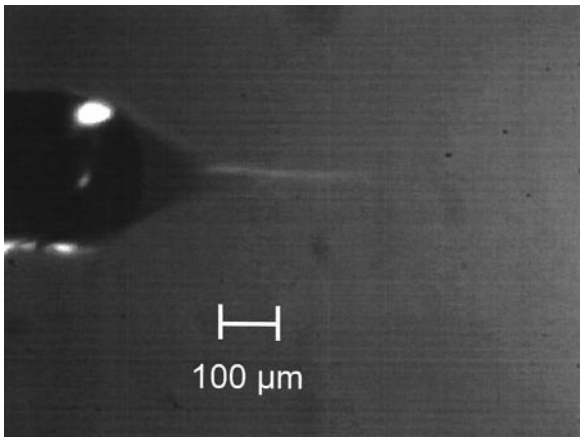

Fig. 7. Microphotograph of the liquid cone in the axial spray mode II obtained under continuous illumination (translumination) with H_2O/MeOH (1:1), U_{cap} = 2.5 kV, I_{coll} = 45 nA and ν_{puls} = 1.9 kHz.

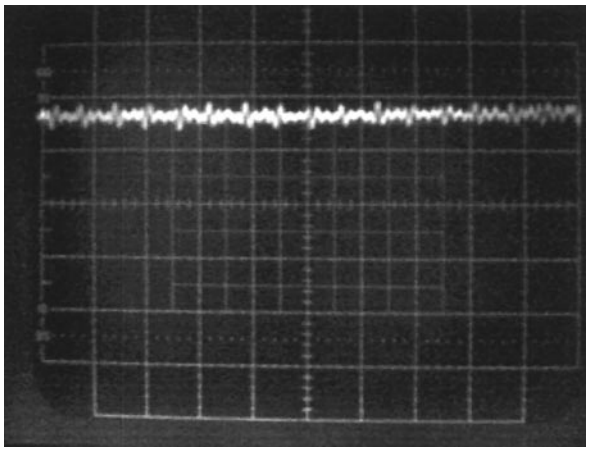

Fig. 8. Capillary current vs. time oscillograms obtained in the axial spray mode III with H_2O/MeOH (1:1), U_{cap} = 3.2 kV, I_{coll} = I_{cap} = 120 nA; y-axis, 2 nA/div.; x-axis, 10 μs/div.

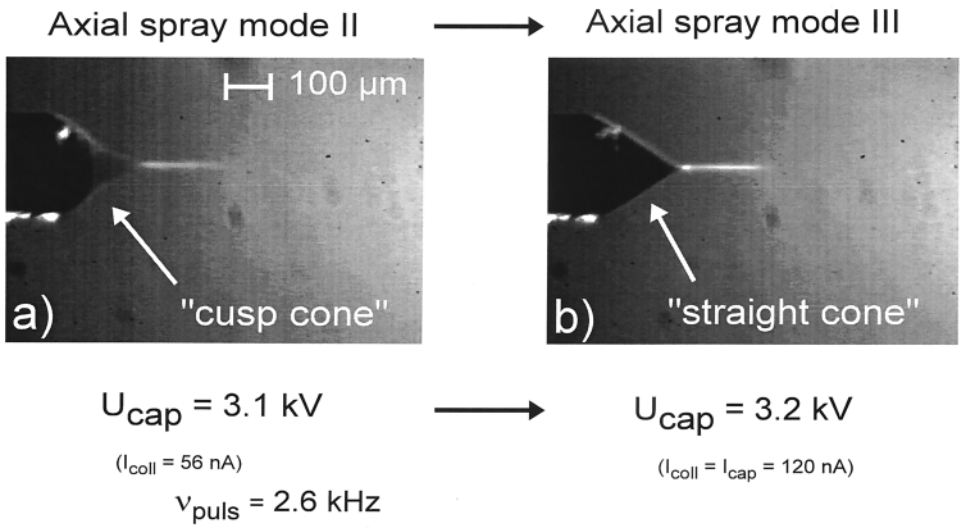

Fig. 9. Microphotographs of the liquid cone obtained under continuous illumination (translumination) at the transition from the axial spray mode II (a) to the axial spray mode III (b) with H_2O/MeOH (1:1).

volume is subjected to this imbalance (Fig. 10). After an emission pulse sequence the cone volume is small and the radius of curvature at the apex large. The cone volume is continuously built up by the supply of liquid maintained by the syringe pump until the radius of curvature (R) of the liquid surface at the cone apex decreases below a critical value (R_{crit}) at which the Maxwell stress, i.e. the outward electrostatic pressure

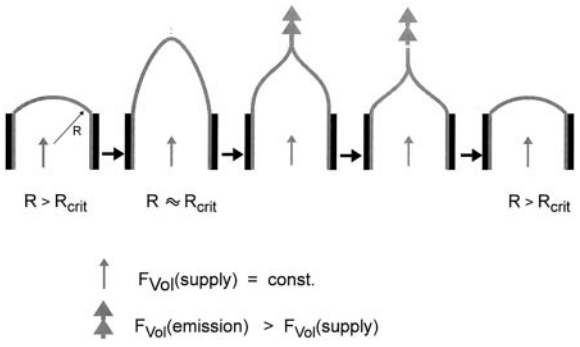

Fig. 10. Schematic representation of the dependence of a "low" frequency pulsation cycle on the imbalance between the loss of liquid by a sequence of "high" frequency emission pulses and the supply of liquid to the cone volume. R is the radius of curvature of the liquid surface at the cone apex; F_{vol}(supply), the constant liquid supply rate to the cone volume; and F_{vol}(emission), the liquid emission rate.

(p_{Max}), exceeds the surface tension forces, i.e. capillary pressure (p_{cap}), for the breakup of the surface and the formation of a liquid jet:

$$p_{Max} = 1/2 \cdot \epsilon_0 E^2 > 2\gamma/R = p_{cap}$$

where E is the electric field strength at the apex of the cone and γ the surface tension of the liquid. During the following pulse sequence the liquid is intermittently emitted at an average emission rate exceeding the liquid supply rate roughly by a factor of 2. As a consequence of the liquid emission the cone volume decreases and the critical radius necessary for liquid emission via high frequency pulsations is finally exceeded. Because of the continuous liquid supply from the capillary the cone volume increases again and the cycle repeats.

The appearance of single liquid emission pulses with a "high" repetition frequency is due to an imbalance between the supply and the loss of liquid in the cone apex region. As schematically shown in Fig. 11, the supply of liquid into the cone apex decreases the radius of surface curvature at the cone apex up to a critical value where the Maxwell stress exceeds the capillary pressure and a jet is formed. Because the loss rate of liquid is higher by a factor of about two

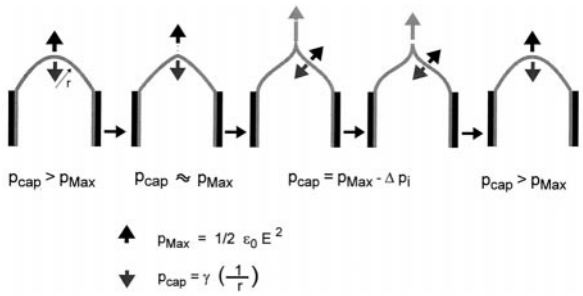

Fig. 11. Schematic representation of the dependence of a single high frequency pulsation cycle on the imbalance between the loss of liquid by a single emission pulse and the liquid supply to the cone apex. *R* is the radius of curvature of the liquid surface at the points indicated by the arrows.

than the supply rate of liquid into the cone apex, the cusp shape of the cone increases with time. Accordingly the Maxwell stress on the cone surface near the apex decreases and the capillary pressure increases. In addition, the high velocity of the liquid near the cone apex reduces the pressure in the liquid and thus the effect of the Maxwell stress by a term Δp_i (Fig. 11). After the loss of a critical amount of liquid the jet tears off and the liquid surface relaxes to its equilibrium shape in the external field. An additional supply of liquid to the cone apex again decreases the radius of curvature and leads to the formation of a cone jet, i.e. the cycle repeats. With increasing capillary potential the Maxwell stress increases and accordingly the cone volume subjected to pulsed emission decreases [17], which causes the increase of the pulsation frequency. In the transition from the spray mode I to II the loss of liquid in a single emission pulse cycle equals the supply of liquid to the cone apex. This condition automatically holds at higher potentials by an appropriate rise of the pulsation frequency.

If at higher capillary potentials the continuous supply rate of the liquid equals the loss rate of the liquid via the cone jet, the transition to the spray mode III occurs. In the potential range of a continuous emission of a liquid via a cone jet the liquid emission rate remains constant but the jet diameter decreases and the jet velocity increases with increasing potential.

The charge carried off with the jet depends more strongly on the duty cycle of its appearance than on the emitted liquid volume, which remains constant in average. Hence, the sudden increase of the average current by a factor of two with the transition from mode II to III fits the increase in duty cycle from ~50% to 100%. This supports a remark made by Fernandez de la Mora and Loscertales [21] that a cone jet may be regarded as a constant-current generator.

The disintegration of a cone jet into droplets is not well understood [22–26]. For conditions of lower field strengths, i.e. lower surface charging of a jet, the breakup of a jet into droplets is attributed to the effect of surface waves [11]. Surface waves propagating along the surface of a jet are generated by disturbances of the jet. Because the amplitude of surface waves of an appropriate wave length ("varicose waves") is enhanced by surface tension forces they lead to the breakup of a cylindrical jet with radius α into droplets of radius $r = 1.89\ \alpha$. This mechanism is well established for uncharged jets and was first described by Rayleigh [27]. The effect of surface charging on this mechanism is not yet clear. Under the conditions of ESMS the generation of varicose waves should not play a major role in the breakup of a cone jet into droplets. Considering the growth of an electrically conducting liquid jet from the apex of a cone formed after an emission pulse the field strength at the tip of the jet increases with the length of the jet because of a decrease of the electrical field shielding by the large outer diameter of the capillary and in addition because of a decrease of the diameter of the accelerated jet, which behaves as a vena contracta [28]. This corresponds to an increasing field stress at the tip of the jet in the direction toward the counter electrode. For these conditions a high field stress also exists on the surface of the jet close to the apex of the tip, i.e. perpendicular to the direction of the jet, with a strong gradient toward the apex. The high field stress reduces the effect of surface tension forces, i.e. of the capillary pressure in the apex region, a flow of liquid to the apex is induced. This should lead to the formation of a highly charged droplet by the relaxation of the adjacent less charged surface of the liquid jet. After removal of the droplet this mechanism

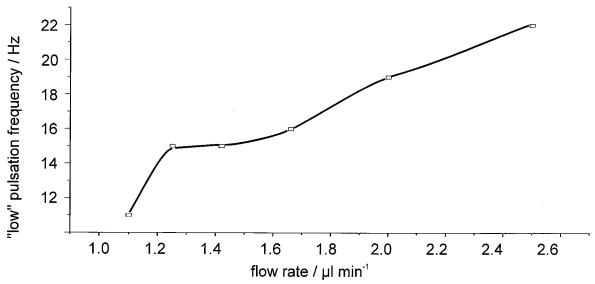

Fig. 12. "Low" pulsation frequency (due to the appearance of pulse sequences) vs. flow rate in the axial spray mode I with H_2O/MeOH (1:1) and U_{cap} = 2.2 kV.

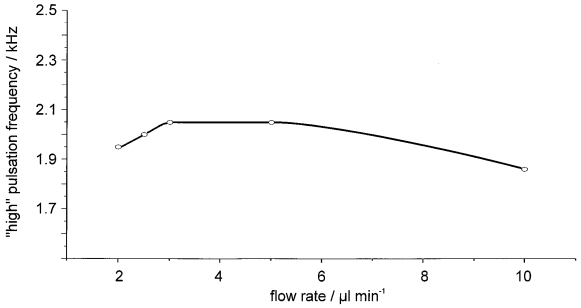

Fig. 13. "High" pulsation frequency (due to the appearance of single pulses) vs. flow rate in the axial spray mode II with H_2O/MeOH (1:1) and U_{cap} = 2.5 kV.

repeats, probably with a frequency of some megahertz, and should produce a mist of nearly monodisperse droplets. It affects the capillary current only weakly and is probably not detectable by a pulsation frequency. This mechanism will be discussed in more detail elsewhere. It may be added that in electrospray the release of charged droplets directly from the apex of a cone is not possible in competition with the formation of a cone jet and accordingly has not been observed.

3.4. Effect of experimental parameters on capillary current pulsations

Besides the capillary potential, the important parameters that are subject to changes in ESMS praxis are the liquid flow rate, the electrolyte concentration, the surface tension of the liquid, which varies with its composition, and the diameter of the spraying capillary, which is greatly reduced in nanoelectrospray mass spectrometry [29,30].

3.4.1. Liquid flow rate

If a change of spray mode is to be avoided the flow rate can only be varied in a limited range. In the axial spray mode I the "low" frequency of the appearance of current pulse sequences increases with the liquid flow rate (Fig. 12). This can be explained by the fact that because of the increase in flow rate a shorter time is needed to build up the required large cone volume with a critical radius for the onset of a liquid emission process. The number of pulses in a sequence also slightly increases with flow rate because the raised liquid supply extends the emission time.

The "high" pulsation frequency in the spray mode I and II shows only a weak dependence on the liquid flow rate (Fig. 13). This is consistent with a minor dependence of "high" frequency pulsations on the liquid supply to the bulk of the cone. The observed increase of the pulse amplitude and width and accordingly of the duty cycle of the "high" frequency pulsation with flow rate can be attributed to an effect of the liquid supply to the apex region of the cone.

3.4.2. Electrolyte concentration in the liquid

The electrolyte concentration was varied between 10^{-8} and 10^{-2} M by adding KBr to the solution of H_2O/MeOH (1:1). This concentration range corresponds to an electrical conductivity between 10^{-5} and 0.55 S/m. Fig. 14 shows the dependence of "low" and "high" frequency pulsations on the electrolyte concentration for different capillary potentials and at a constant flow rate (2 μL/min). Both pulsation frequencies increase weakly with the concentration of the electrolyte. Accordingly, the capillary potential at which the transition from axial spray mode I to mode II occurs decreases by the addition of the electrolyte (Fig. 14). The weak increase of the pulsation frequencies indicates that the electrohydrodynamic processes are only weakly affected by the change in the electrolyte concentration. The dielectrical relaxation time

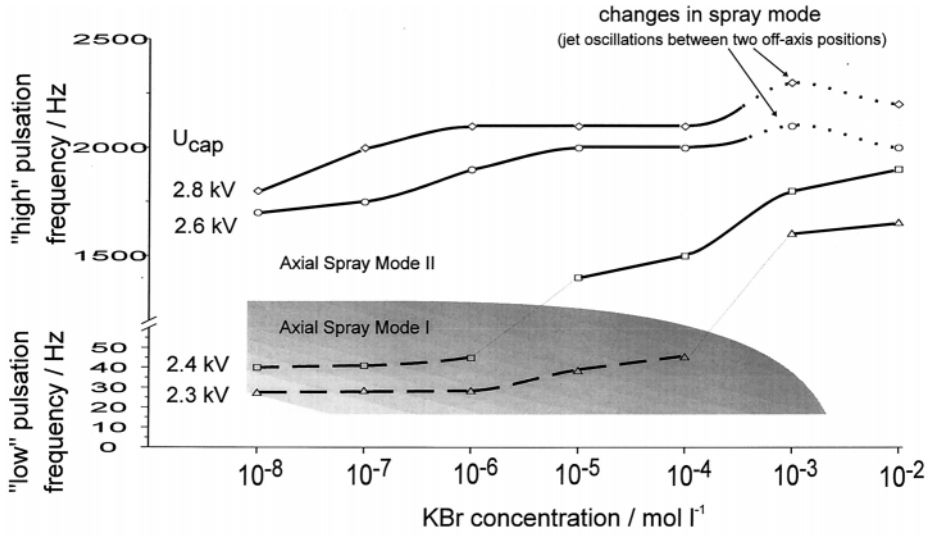

Fig. 14. "Low" and "high" pulsation frequencies vs. KBr concentration in H_2O/MeOH (1:1) for different capillary potentials.

of the pure solvent (H_2O/MeOH) is already short ($\tau =$ 17 μs) compared with the time scale of a single pulse period. Therefore, the charge rearrangement at the surface of the liquid cone follows the fluid mechanics rather instantaneously.

The measured average capillary current increases with increasing electrolyte concentration. Hence, the charge that is emitted during a single pulse increases from about $2.3 \cdot 10^{-11}$ C for the 10^{-8} M KBr solution to $6 \cdot 10^{-11}$ C for the 10^{-2} M KBr solution. For a given electrolyte concentration the emitted charge per pulse is nearly independent of the applied capillary potential in the axial spray mode II, as mentioned before.

At KBr concentrations above 10^{-3} M the spray mode itself changes. In the higher potential range of the axial spray mode II the pulsating liquid jet leaves its axial orientation and oscillates between two off-axis positions (Fig. 15). The measured pulsation frequency (marked by dotted lines in Fig. 14) is close to that observed in the axial spray mode II. Flash microphotography revealed that the jet appears only at one of the two off-axis positions during a single current pulse. With the experimental setup used it was not possible to correlate a shape of a current pulse with the corresponding jet position. It is probable that the jet position alternates from pulse to pulse.

3.4.3. Surface tension of the liquid

The surface tension was varied by addition of Triton X-114 to the solution of H_2O/MeOH in the concentration range between 10^{-8} and 10^{-1} M. Triton X-114 consists of a mixture of octylphenolpolyglycolethers (OPE) with a distribution maximum at 7–8 ether groups. As a nonionic surfactant, it does not significantly influence the conductivity of the liquid. In Fig. 16 the dependence of "high" frequency pulsa-

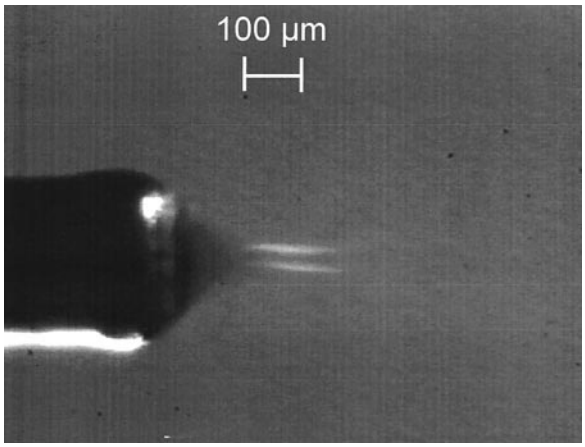

Fig. 15. Microphotograph obtained under continuous illumination (translumination) of the liquid cone showing the oscillation of the jet between two off-axis positions with 10^{-3} M KBr in H_2O/MeOH (1:1) and $U_{cap} = 2.8$ kV.

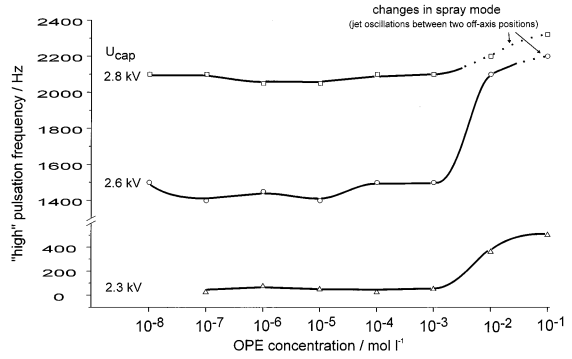

Fig. 16. "High" pulsation frequency vs. surfactant concentration for different capillary potentials with nonionic surfactant Triton X-114 (OPE) in H_2O/MeOH (1:1).

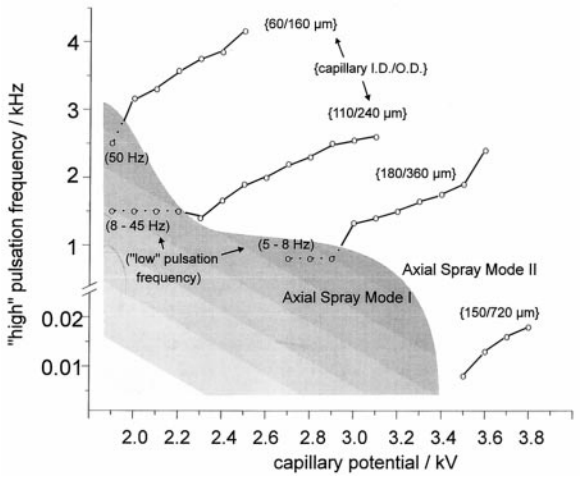

Fig. 17. "High" pulsation frequency vs. capillary potential for capillaries of different diameters (i.d./o.d.) with H_2O/MeOH (1:1) and a flow rate of 2 μL/min. The observed "low" pulsation frequencies in the axial spray mode I are indicated.

tions on the surfactant concentration is shown for different capillary potentials and at a constant flow rate (2 μL/min). The pulsation frequency remains almost unaffected by the surfactant in the concentration range from 10^{-8} to 10^{-3} M. With concentrations exceeding this range a significant increase in the pulsation frequency is observed. At lower capillary potentials and at surfactant concentrations $>10^{-7}$ M the liquid emission already starts in the axial spray mode II. No distinguishable sequences of emission pulses were observed. Because a lowering of the surface tension has the same effect as an increase of the Maxwell stress, i.e. the capillary potential, the pulsation frequency should increase with the addition of the surfactant. However, on the time scale of the pulsation frequency a rather high surfactant concentration is required for the repeated formation of a surfactant layer at the apex of the liquid cone by diffusion of molecules from the bulk to the surface of the liquid. Accordingly, the pulsation frequency only increases at rather high surfactant concentrations. The suppression of the spray mode I already at low surfactant concentrations is probably related to a weak reduction of the surface tension of the liquid cone. This is only needed for a reduction of the cone length and thereby of the cone volume subjected to pulsed emission.

Similarly at high electrolyte concentrations, high surfactant concentrations lead to oscillations of the jet between two off-axis positions (Fig. 15). This indicates that surface tension effects are probably responsible for these oscillation phenomena.

3.4.4. Diameter of the spraying capillary

Fig. 17 shows the dependence of the capillary potential range in which current pulsations are observed, and the dependence of the pulsation frequencies of the spray mode I and II on the i.d./o.d. of the capillary tip at a constant flow rate of 2 μL/min. With decreasing outer capillary diameter the capillary potential decreases and the pulsation frequencies increase. This dependence can be explained by the increase of the field strength and of the resulting electrostatic forces on the liquid at the end of the capillary with decreasing outer diameter.

The electrospray process under nanoelectrospray conditions was investigated by using drawn glass capillaries with i.d./o.d. of 0.5/1 μm. The distance between the capillary tip and the counter electrode was about 2 mm and the capillary potential applied was 700 V. The liquid was not supplied by a syringe pump but pulled out by electrostatic forces. The experimental conditions were similar to those reported by Wilm and Mann [29,30]. For these conditions of ESI a capillary current of about 10 nA with a noise level of 1–2 nA was measured and no current

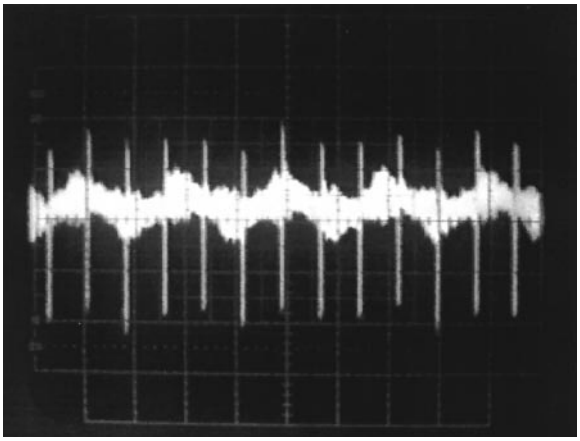

Fig. 18. Capillary current vs. time oscillogram obtained under nanospray conditions for U_{cap} = 2.0 kV and I_{coll} = 20 nA, y-axis, 2 nA/sca.div.; *x* axis, 10 ms/div.

pulsation phenomena were observed. Current pulsations only appeared under conditions of a (corona) discharge, i.e. after raising the capillary potential to high values. Fig. 18 shows a capillary current versus time oscillogramm obtained at a capillary potential of 2.0 kV with a H_2O/MeOH (1:1) solution. Current pulsations with a frequency of about 130 Hz were observed. The frequency increased with the capillary potential. The pulsations differ significantly from those observed in the axial spray mode II. The current first decreases from a noisy level, but not to zero, then increases above and decreases again to the "permanent" noisy level. This behavior is probably related to the formation of a droplet at the end of the capillary tip, which interrupts the discharge, and to the subsequent emission of this droplet, which leads to a short current pulse and the onset of discharge again. For these conditions optical observations were not possible.

3.5. Effect of capillary current pulsations on ESMS

Capillary current pulsations are correlated with the intermittent emission of charged droplets via a cone jet. As mass spectrometric detectable ions are released from these droplets ESI is a discontinuous process in the axial spray modes I and II. This is easily observed by mass spectrometry for the axial spray mode I by "low" frequency pulsations of the ion signal (Fig. 19). The "high" frequency pulsations of ion signals are less obvious because the peaks are broadened by the more or less delayed release of ions from charged droplets and the passage of the ions through the atmospheric pressure interface of an ESMS. Fig. 20 shows a two channel oscillogram obtained in the axial spray mode II during ESMS of a solution of 10^{-3} M $BaBr_2$ in H_2O/MeOH (1:1). The upper trace shows the time dependence of the Ba^{2+} signal at the electron multiplier detector and the lower trace the time

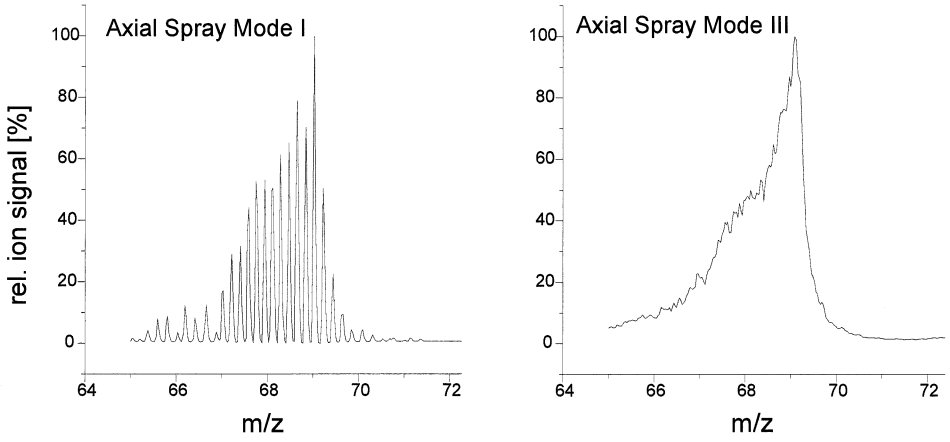

Fig. 19. Single mass scans of Ba^{2+} signals at low resolution from m/z = 65–72 with 0.5 s/u in the axial spray mode I and III; solution, 10^{-3} M $BaBr_2$ in H_2O/MeOH (1:1).

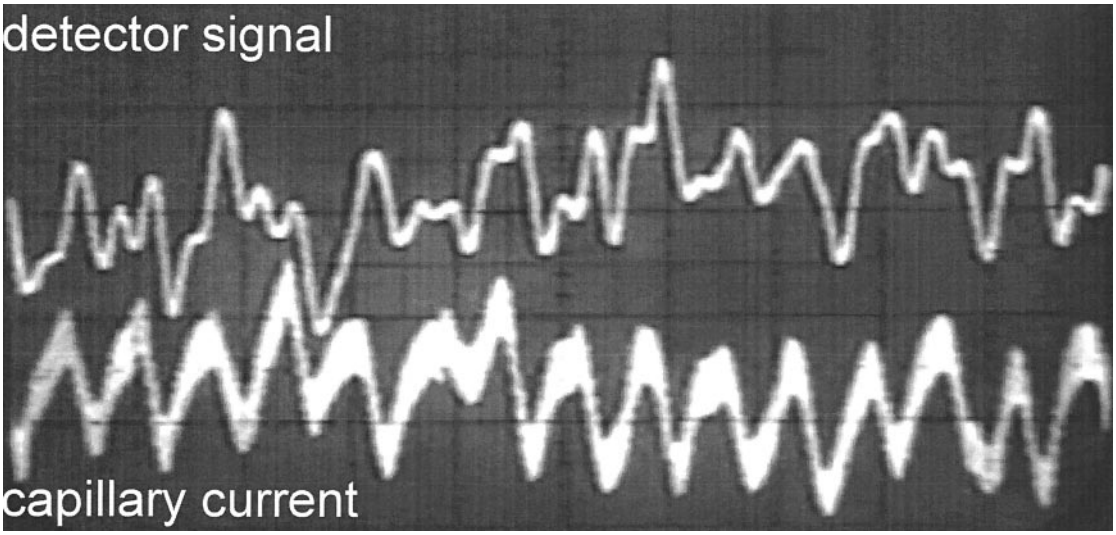

Fig. 20. Detector signal at $m/z = 69$ (Ba^{2+}) and capillary current vs. time (1 ms/div.) oscillogram obtained during ESMS of a solution of 10^{-3} M $BaBr_2$ in H_2O/MeOH (1:1) in the axial spray mode II with $U_{cap} = 2.4$ kV.

dependence of the corresponding capillary current. The signal originating from the spraying capillary is rather distorted compared with the signals that are obtained with the experimental setup for optical observations. This is mainly due to the limited possibility of electrically shielding of the ESMS setup so that the capillary current signal had to be passed through high- and low-pass filters. In addition, the optoelectronic coupling circuit necessary for floating the spraying capillary at a high electrical potential led to distortions of the peak shape. However, it can be seen that the pulsations of the detector signal correspond to the pulsations of the capillary current. The oscillations of the detector signal have no direct consequences for ESMS at slow mass scan rates or if a spectrum is accumulated from many single scans. However, for fast scans or in ESI time-of-flight (TOF) mass spectrometry, where an ion "bunch" is separated for TOF analysis by a short orthogonal extraction pulse [31], the pulsed emission of liquid has to be considered.

The dependence of the average ion signal intensity on the axial spray modes is shown in Fig. 21 for the same solution. The (average) ion signal intensity does not continuously increase with the (average) capillary current but shows a local maximum in the transition range between the axial spray mode I and II that is not reflected in the capillary current. This maximum can be attributed to the dispersion of the liquid into fine and highly charged droplets. Considering the duty cycle of the pulsed emission, the local maximum of the ion signal corresponds to a maximum ionization efficiency, defined as the ratio of the signal intensity to the capillary current. Accordingly, the maximum signal intensity is obtained in the spray mode III, i.e. at higher capillary potential, but this does not corre-

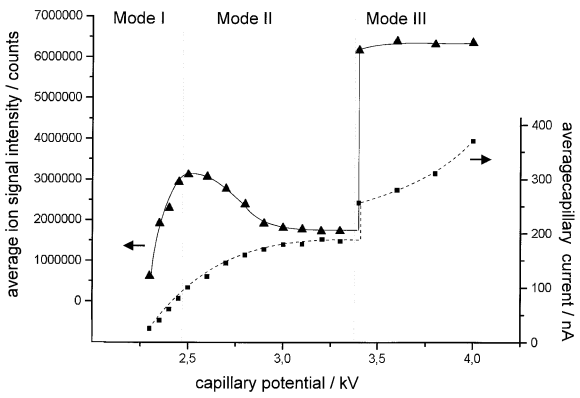

Fig. 21. Average total ion signal intensity and average capillary current vs. capillary potential obtained during ESMS of a solution of 10^{-3} M $BaBr_2$ in H_2O/MeOH.

spond to the highest ionization efficiency. Separate experiments with a TOF mass analyser revealed that the ionization efficiency is higher at the beginning than at the end of an emission pulse because of a decreasing size of the charged droplets formed [32].

These results show that for optimum use of ESMS in analytical applications the actual spray mode and the pulsation phenomena have to be considered. The measurement of the capillary current provides a means to select a spray mode and to monitor the ESI conditions without the need for optical observations.

Acknowledgement

Support of this work by the Deutsche Forschungsgemeinschaft is gratefully acknowledged.

References

[1] M. Yamashita, J.B. Fenn, J. Phys. Chem. 88 (1984) 4451.
[2] M.L. Alexandrov, L.N. Gall, N.V. Krasnov, V.I. Nikolaev, V.A. Pavlenko, V.A. Shkurov, Dokl. Akad. Nauk SSSR 277 (1984) 379.
[3] M. Dole, L.L. Mack, R.L. Hines, R.C. Mobley, L.D. Ferguson, M.B. Alice, J. Chem. Phys. 49 (1968) 2240.
[4] (a) J.V. Iribarne, B.A.J. Thomson, Chem. Phys. 64 (1976) 2287. (b) B.A.J. Thomson, J.V. Iribarne, J. Chem. Phys. 71 (1979) 4451.
[5] K.W.M. Siu, R. Guevremont, J.C.Y. Le Blanc, R.T. O'Brian, S.S. Berman, Org. Mass Spectrom. 28 (1993) 579.
[6] (a) F.W. Röllgen, E. Bramer-Weger, L. Büttfering, J. Phys. Colloq. 48 (1987) C6-253. (b) G. Schmelzeisen-Redeker, L. Büttfering, F.W. Röllgen, Int. J. Mass Spectrom. Ion Processes 90 (1989) 139.
[7] J.B. Fenn, J. Am. Soc. Mass Spectrom. 4 (1993) 524.
[8] I.G. Loscertales, J. Fernandez de la Mora, J. Chem. Phys. 103 (1995) 5041.
[9] P. Kebarle, L. Tang, Anal. Chem. 65 (1995) 972A.
[10] F.W. Röllgen, U. Lüttgens, Th. Dülcks, U. Giessmann, Proc. ASMS Conf., San Francisco, 1993, p. 1.
[11] A.G. Bailey, Electrostatic Spraying of Liquids, Wiley, New York, 1988.
[12] J.M. Grace, J.C.M. Marijnissen, J. Aerosol Sci. 25 (1994) 1005.
[13] M. Cloupeau, B. Prunet-Foch, J. Aerosol Sci. 25 (1994) 1021.
[14] U. Lüttgens, F.W. Röllgen, K.D. Cook, in: K. Standing, W. Ens (Eds.), Methods and Mechanisms for Producing Ions from Large Molecules, Plenum, New York, 1991, p. 185.
[15] S.B. Sample, R. Bollini, J. Coll. Sci. 41 (1972) 185.
[16] D. Chen, D.Y.H. Pui, S.L. Kaufmann, J. Aerosol Sci. 26 (1995) 963.
[17] I. Hayati, A.I. Bailey, T.F. Tadros, J. Coll. Sci. 117 (1987) 205.
[18] G. Taylor, Proc. R. Soc. A280 (1964) 383.
[19] F. Charbonnier, C. Rolando, F. Saru, P. Hapiot, J. Pinson, Rapid Commun. Mass Spectrom. 7 (1993) 707.
[20] Th. Dülcks, F.W. Röllgen, J. Mass Spectrom. 30 (1995) 324.
[21] J. Fernandez de la Mora, I.G. Loscertales, J. Fluid Mech. 260 (1994) 155.
[22] K. Kim, R.J. Turnbull, J. Appl. Phys. 47 (1976) 1964.
[23] R.L. Hines, J. Appl. Phys. 37 (1966) 2730.
[24] D.W. Horning, C.D. Hendricks Jr., J. Appl. Phys. 50 (1979) 2614.
[25] A.B. Basset, Am. J. Math. 16 (1894) 93.
[26] J.M. Schneider, N.R. Lindblad, C.D. Hendricks, J.M. Crowley, J. Appl. Phys. 38 (1967) 2599.
[27] Lord Rayleigh, Proc. R. Soc. 29 (1879) 71.
[28] R.G. Forbes, J. de Phys. IV, 6-C5 (1996) 43.
[29] M. Wilm, M. Mann, Int. J. Mass Spectrom. Ion Processes 136 (1994) 167.
[30] M. Wilm, M. Mann, Anal. Chem. 68 (1996) 1.
[31] A.N. Verenchikov, W. Ens, K.G. Standing, Anal. Chem. 66 (1994) 126.
[32] R. Juraschek, A. Schmidt, M. Karas, F.W. Röllgen, Proc. 14th IMSC, Tampere, 1997, in press.